Available online at www.springerlink.com

Acta Metall. Sin. (Engl. Lett.) Vol.26 No. 2 pp. 157—166 April 2013

ACTA
METALLURGICA SINICA
(ENGLISH LETTERS)

Wear Behavior of Cold Pressed and Sintered Al_2O_3/TiC/CaF_2-Al_2O_3/TiC Laminated Ceramic Composite

Xuefeng YANG[1)†], Jian CHENG[2)], Peilong SONG[1)], Shouren WANG[1)], Liying YANG[1)], Yanjun WANG[1)] and Ken MAO[3)]

1) School of Mechanical Engineering, University of Jinan, Jinan 250022, China

2) Key Laboratory for Anisotropy and Texture of Materials of the Ministry of Education, Northeastern University, Shenyang 110089, China

3) School of Engineering, Warwick University, Coventry, CV4 7AL, UK

[Manuscript received 10 December 2012, in revised form 8 January 2013]

A novel laminated Al_2O_3/TiC/CaF_2-Al_2O_3/TiC sandwich ceramic composite was fabricated through cold pressing and sintering to achieve better anti-wear performance, such as low friction coefficient and low wear rate. Al_2O_3/TiC/CaF_2 and Al_2O_3/TiC composites were alternatively built layer-by-layer to obtain a sandwich structure. Solid lubricant CaF_2 was added evenly into the Al_2O_3/TiC/CaF_2 layer to reduce the friction and wear. Al_2O_3/TiC ceramic was also cold pressed and sintered for comparison. Friction analysis of the two ceramics was then conducted via a wear-and-tear machine. Worn surface and surface compositions were examined by scanning electron microscopy and energy dispersion spectrum, respectively. Results showed that the laminated Al_2O_3/TiC/CaF_2-Al_2O_3/TiC sandwich ceramic composite has lower friction coefficient and lower wear rate than those of Al_2O_3/TiC ceramic alone because of the addition of CaF_2 into the laminated Al_2O_3/TiC/CaF_2-Al_2O_3/TiC sandwich ceramic composite. Under the friction load, the tiny CaF_2 particles were scraped from the Al_2O_3/TiC/CaF_2 layer and spread on friction pairs before falling off into micropits. This process formed a smooth, self-lubricating film, which led to better anti-wear properties. Adhesive wear is the main wear mechanism of Al_2O_3/TiC/CaF_2 layer and abrasive wear is the main wear mechanism of Al_2O_3/TiC layer.

KEY WORDS: Friction and wear characteristics; Wear property; Ceramic-matrix composites; Layer manufacture; Surface appearance; Sliding

1. Introduction

Self-lubrication of friction surfaces, which enhances wear resistance and reduces friction coefficients, is currently an area of enhanced interest in materials science. Self-lubrication improves wear resistance of materials and reduces maintenance cost[1]. Self-lubrication is one of the most widely used methods for forming a new reparative film on the surface of a friction pair[2]. A self-lubricating effect can be identified by either physical or chemical process (or both) in a friction system[3−5].

† Corresponding author. Assoc. Prof., Ph.D.; Tel: +86 531 82765870; E-mail address: me_yangxf@ujn.edu.cn (Xuefeng YANG)

DOI: 10.1007/s40195-012-0247-5

Ceramics have excellent mechanical properties such as the wear resistance, oxidation resistance, and corrosion resistance[6−8]. A number of researchers have argued that the abrasive and adhesive wears are the predominant wear mechanisms on the wear surface of friction pairs for ceramic materials[9−11].

CaF_2 is a well-known, widely used solid lubricant which has physical, chemical, and microstructural influences on the tribological contact of working surface. The mechanism of the effective lubricating performance of CaF_2 is easy shearing along the basal plane of the hexagonal crystalline structure because of its lamellar structure and low shear strength. In addition, CaF_2 is a useful addition in the production of self-lubricating ceramic composites, and is used in different anti-wear applications. In earlier studies[12−15], a number of ceramic composites, such as Al_2O_3/CaF_2, SiC/CaF_2, and Al_2O_3/TiC/CaF_2 have been developed. Tribological and microstructural studies have also been extensively conducted on these composites and their mechanical properties. The addition of solid lubricants to the ceramic matrix can improve its tribological properties.

In this article, Al_2O_3/TiC/CaF_2-Al_2O_3/TiC laminated ceramic composite and Al_2O_3/TiC ceramic are developed via cold pressing and sintering to study friction coefficients and wear rates according to self-lubricating theory[16–23]. Wear-and-tear behaviors of Al_2O_3/TiC/CaF_2-Al_2O_3/TiC laminated ceramic composite and Al_2O_3/TiC ceramic are investigated and revealed also. their self-lubricating effect and wear-resistance characteristics.

2. Experimental

2.1 Specimen preparation and its mechanical properties

Sandwich-like structure of the laminated ceramic composite and Al_2O_3/TiC ceramic were fabricated via cold pressing and sintering to obtain self-lubrication. The designed laminated Al_2O_3/TiC/CaF_2-Al_2O_3/TiC composite structure is shown in Fig. 1. The laminated Al_2O_3/TiC/CaF_2 and Al_2O_3/TiC with a sandwich-like structure were built layer by layer to obtain the predefined dimension. Raw material for the specimen sintering was composed of Al_2O_3, TiC, CaF_2, Mo and Ni. Density of α-Al_2O_3 powder was 3.99 g/cm^3 and its purity was more than 99.9% with an average diameter $\leq$2 μm. Density of TiC was 4.25 g/cm^3 and its purity was 99.8% with an average diameter $\leq$2 μm. Density of CaF_2 was 3.18 g/cm^3 and its purity was more than 98.5%. The aforementioned powders were mixed with pure water and a small ceramic ball in a planetary ball milling canister for 120 h. Phase contents of the Al_2O_3/TiC layer were 45 vol.% Al_2O_3 and 55 vol.% TiC. Small amounts of Mo and Ni powders were added to the mixture to strengthen the matrix. The self-lubricating Al_2O_3/TiC/CaF_2 layer was then prepared using Al_2O_3, TiC, and CaF_2, with their phase contents being 67.5 vol.%, 22.5 vol.%, and 10 vol.%, respectively. Raw material preparation of Al_2O_3/TiC ceramic was identical to the Al_2O_3/TiC layer of the aforementioned laminated composite.

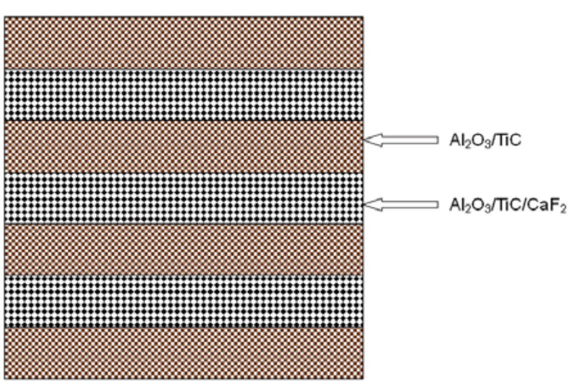

Fig. 1 Schematic of the laminated sandwich-structure-like Al_2O_3/TiC/CaF_2-Al_2O_3/TiC ceramic composite

After being heated in a dry box, the mixed powders were sifted through a screen under flowing N_2 atmosphere. The laminated sandwich composite and Al_2O_3/TiC ceramic were then fabricated via cold pressing and sintering. Graphite mold suitable for preparing ceramic composites was designed. Sintering temperature was set at (1750±33) °C and cold pressure was set at 50 MPa. Al_2O_3/TiC/CaF_2 and Al_2O_3/TiC powders of the prepared specimen were in turn placed in the graphite mold. Heating cycle was 10 minutes using Ar as sintering atmosphere. Two specimens were prepared following the aforementioned procedure. Specimens were then sliced into pucks measuring 3 mm×4 mm×36 mm. General mechanical properties of the specimens were evaluated. Density (ρ) of specimens was measured according to $\rho = m/V$, where m is the mass of the specimens which was measured using an electronic scale with a resolution of 0.0001 g, V is the volume of the specimens. Dimensions of the specimens were measured using a micrometer. Hardness was measured using a Vickers sclerometer. Bending strength was measured via a three-point bending test using a span distance of 20 mm and a loading rate of 0.2 mm/min. Fracture toughness was measured using an impress method, with the force of impress being 196 N and retaining time being 15 s. Lengths of cracks were measured under an optical microscope with 400 times magnification. Detailed mechanical properties of the specimens are provided in Table 1. Macrophotograph of Al_2O_3/TiC/CaF_2-Al_2O_3/TiC laminated ceramic composite is shown in Fig. 2. Microstructure and EDS results of Al_2O_3/TiC/CaF_2 are further shown in Fig. 3. Fig. 3(a) shows that the big granules are Al_2O_3 and TiC, CaF_2 particles exist at the gaps of the granules as binding phase because CaF_2 melt at 1450 °C. The EDS results of Al_2O_3, TiC and CaF_2 are shown in Fig. 3(b), (c) and (d), respectively. The mechanical properties and the hardness of Al_2O_3/TiC/

Table 1 Mechanical properties of the Al_2O_3/TiC/CaF_2-Al_2O_3/TiC laminated ceramic composite

Materials	Fracture toughness (MPa·m$^{1/2}$)	Flexure strength (MPa)	Hardness (GPa)	Density (g/cm^3)
Laminated ceramic	2.24	281	6.56	2.88
Al_2O_3/TiC/CaF_2 layer	2.53	321	8.67	2.53
Al_2O_3/TiC layer	1.95	241	4.45	3.13

CaF_2 is better than those of Al_2O_3/TiC because the CaF_2 is used as the binding phase. In sintering processing, the great heat melt CaF_2, and CaF_2 flow into and fill holes. Though CaF_2 has low mechanical properties, CaF_2 replace holes in matrix, and the residual porosity of Al_2O_3/TiC/CaF_2 matrix is less than Al_2O_3/TiC. So the mechanical properties and hardness of Al_2O_3/TiC/CaF_2 is better than Al_2O_3/TiC.

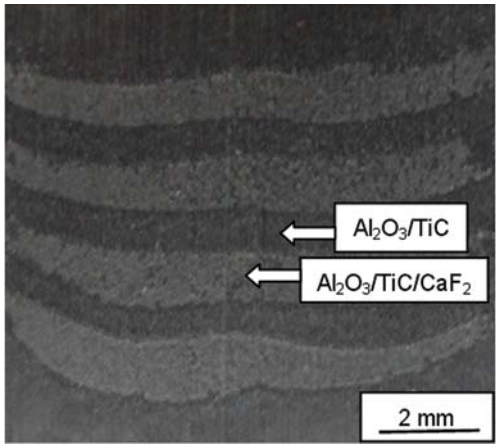

Fig. 2 Cold press and sintered laminated Al_2O_3/TiC/ CaF_2- Al_2O_3/TiC sandwich composite

The ceramic component with CaF_2 addition showed better mechanical properties. Due to the high sintering temperature during the hot sintering, CaF_2 reached its melting point, and flowed into the micro porous gaps of the Al_2O_3/TiC, which worked as an adhesive lead to the improvment of the material's mechanical properties. In the contrary, quite a lot of vacancies exist in the cold sintered ceramic component, which seriously affected the material's mechanical properties. So the hardness of Al_2O_3/TiC layers is lower than Al_2O_3/TiC/CaF_2 layers.

2.2 Experimental setup

Experiment was conducted on an MMG-10 high speed wear-and-tear test machine produced by Jinan Test Machine Co., Ltd. This machine is a pin-on-disc sliding friction type. Ceramic friction coefficient was determined with a given load and rotational speed. After fine polishing, the specimens were fixed tightly onto the machine as a disc source. A ring-shaped quenched 45 steel functioned as the pin and rotational speed of the machine was set between 100 and

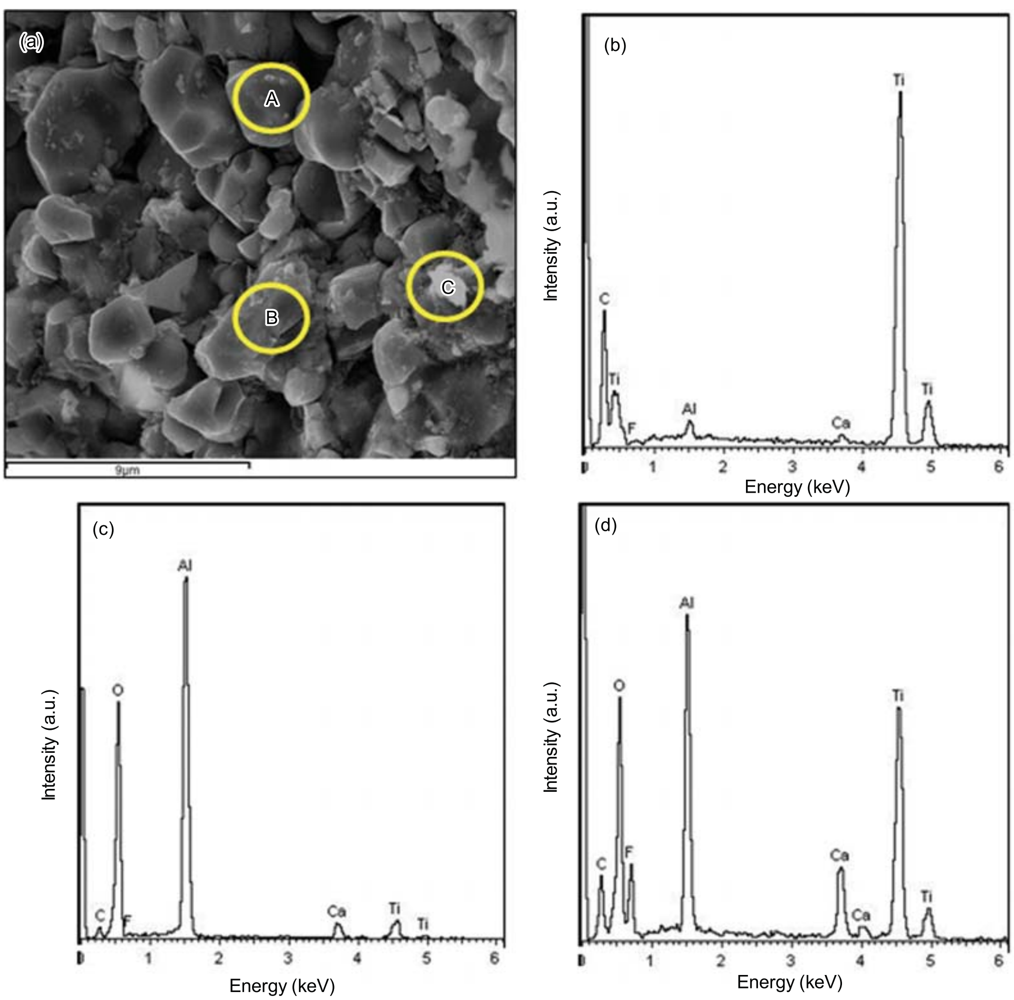

Fig. 3 SEM image of the Al_2O_3/TiC/CaF_2 (a) and EDS results of the position denoted by the circle A (b), circle B (c) and circle C (d) in Fig.3 (a)

400 r/min. The load was applied vertically from top down to the polishing surface of the specimens, ranging from 20 to 100 N. Fig. 4 shows the experimental setup.

Wear and tear of the specimens were calculated based on weight variations of the specimens. During friction-testing procedure, the mass decrease of each specimen was measured using an electronic scale with a 0.001 g precision. The specimens were weighed every 30 min after testing. Wear rate can be calculated using Eq. (1):

$$W = \frac{\Delta\omega}{2\pi Rtn\mu P\rho}, \quad (1)$$

where $\Delta\omega$ is the wear-and-tear mass (g); R stands for average friction radius, which is the distance between the center of the lump and the rotating axis of the ring (m); t is the time duration (min); n is the rotational speed of the ring (r/min); μ is the average friction coefficient; P is the force on the disc (N).

At the end of the experiment, the specimens were washed in an ultrasonic launder using grain alcohol, and then dried and preserved in an air shield environment. Microstructures and energy dispersive spectrum (EDS) analysis of the specimens were carried out under a scanning electronic micrograph.

3. Results and Discussions

3.1 Friction coefficient

Fig. 5 presents the friction coefficient variations with rising load and rotational speed. It is shown that the average friction coefficient of the laminated ceramic composite is irregular. Under the same rotational speed of 100 r/min, the friction coefficient of the specimen increases sharply from 0.3 to approximately 0.6 when the load increases from 20 to 40 N. As the rotational speed further increases, the average friction coefficient only shows a marginal variation between 0.5 and 0.6. This result indicates that the friction coefficient is stabilized between 0.5 to 0.6 with increasing rotational speed and load.

3.2 Wear rate

Wear rate of Al_2O_3/TiC/CaF_2-Al_2O_3/TiC laminated ceramic composites is shown in Fig. 6. When the rotational speed is 100 r/min, the wear rate of the

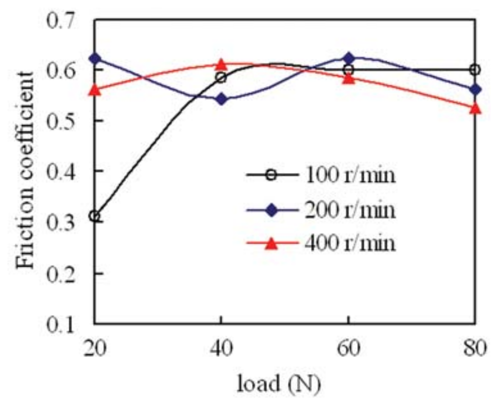

Fig. 5 Friction coefficient of the laminated ceramic composite variation with load and rotational speed

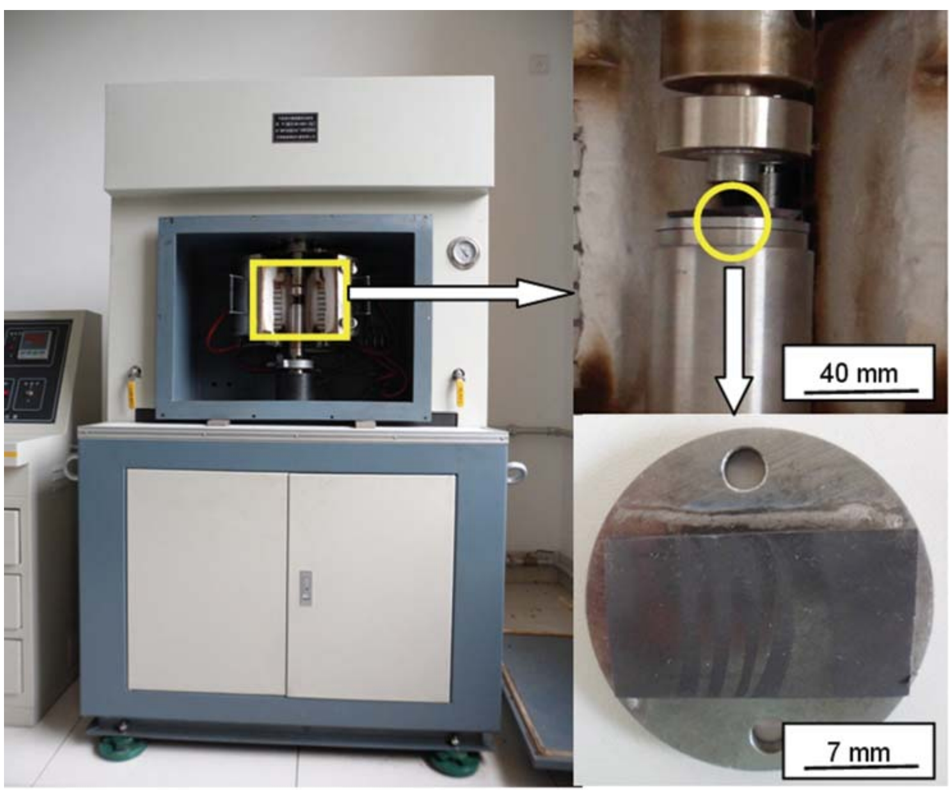

Fig. 4 The experimental setup, the left one is the wear and tear test machine with the right down figure being the tested sandwich ceramic composite surface

laminated ceramic composite is lower than those at 200 r/min and 400 r/min with increasing load, thus indicating a better wear resistance. However, the wear rate of the laminated ceramic composite becomes unstable when the load is increased from 20 to 100 N under a high rotational speed of 400 r/min. Wear rate of the laminated ceramic composite is lower than 10×10^{-11} $m^2\cdot N^{-1}$ when the load is less than 40 N at 400 r/min, and then it increases sharply to more than 30×10^{-11} $m^2\cdot N^{-1}$ when load higher than 60 N. In general, the wear rate of the laminated ceramic composite increases as rotational speed rises. With high rotational speed, the wear rate increases rapidly with the load increasing.

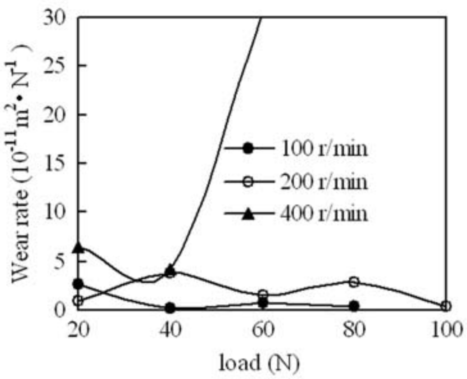

Fig. 6 Wear rate of the laminated Al_2O_3/TiC/CaF_2-Al_2O_3/TiC ceramic composite variation with the load and rotational speed

Table 1 shows that the mechanical properties including fracture toughness, hardness and flexure strength of Al_2O_3/TiC layer are lower than Al_2O_3/TiC/CaF_2 layer. The worn surfaces of the Al_2O_3/TiC/CaF_2 and Al_2O_3/TiC layers were observed by SEM. Fig. 7(a) shows the worn surface of Al_2O_3/TiC/CaF_2, in which some films form on the friction surfaces. Fig. 7(b) shows the EDS of the worn surfaces of Al_2O_3/TiC/CaF_2, and Fe, Ca, F, Ti, C, Al and O are found. Fig. 7(c) shows the micrograph of the worn surface of Al_2O_3/TiC, many small holes are present and the brittle worn sheet is exfoliated from the matrix because of sintering without pressure. Fig. 7(d) shows the EDS of the Al_2O_3/TiC, which exhibiting Ti, C, Al, O, Mo and Ni which all belong to the matrix. The worn surface does not consist of Ca, F and Fe. Al_2O_3/TiC/CaF_2 exhibits adhesive wear mainly because Fe adheres onto the worn surface, and the wear mechanism of Al_2O_3/TiC layer is abrasive wear. Fig. 8 shows the SEM image and EDS result of the worn surface of Al_2O_3/TiC. The Al_2O_3/TiC layer exhibits abrasive wear (Fig. 8(a)). Many furrows and fallen grains are present on the surface. The traces go along the friction direction with heavy wear.

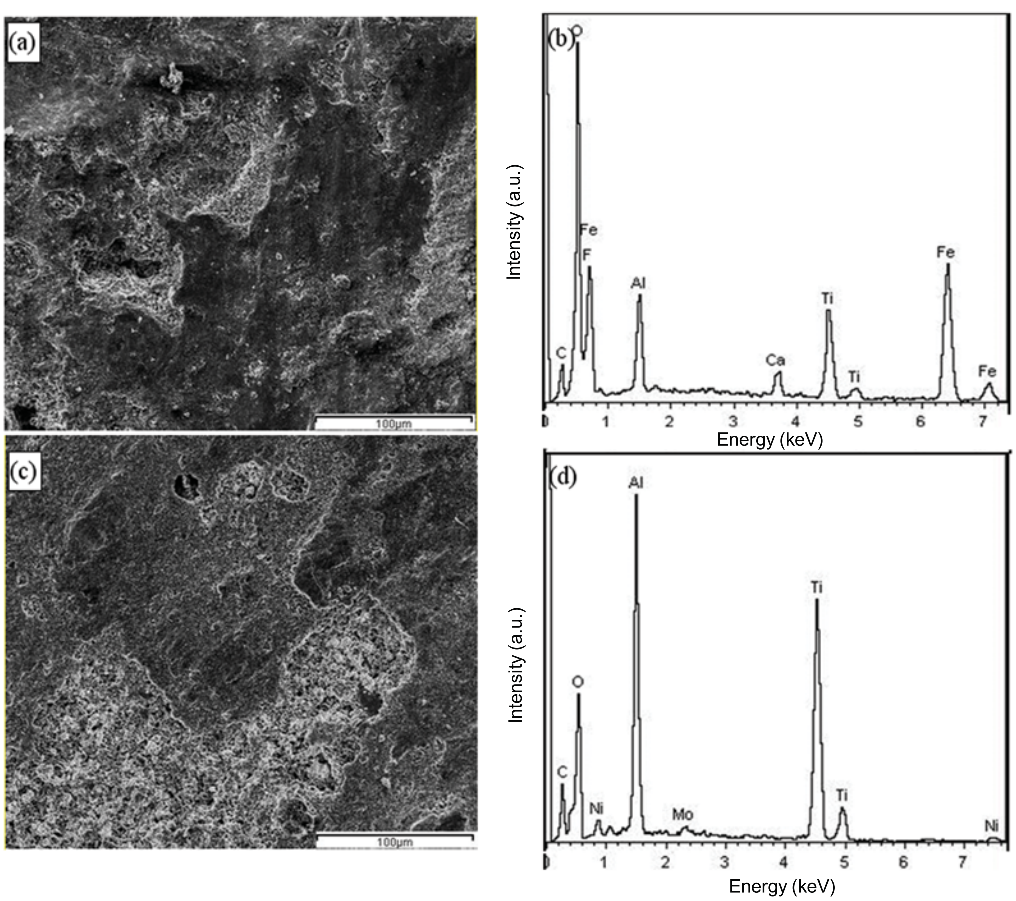

Fig. 7 SEM images and EDS results of the worn surfaces of Al_2O_3/TiC/CaF_2 layer (a, b) and Al_2O_3/TiC layer (c, d) in the laminated Al_2O_3/TiC/CaF_2-Al_2O_3/TiC ceramic composite

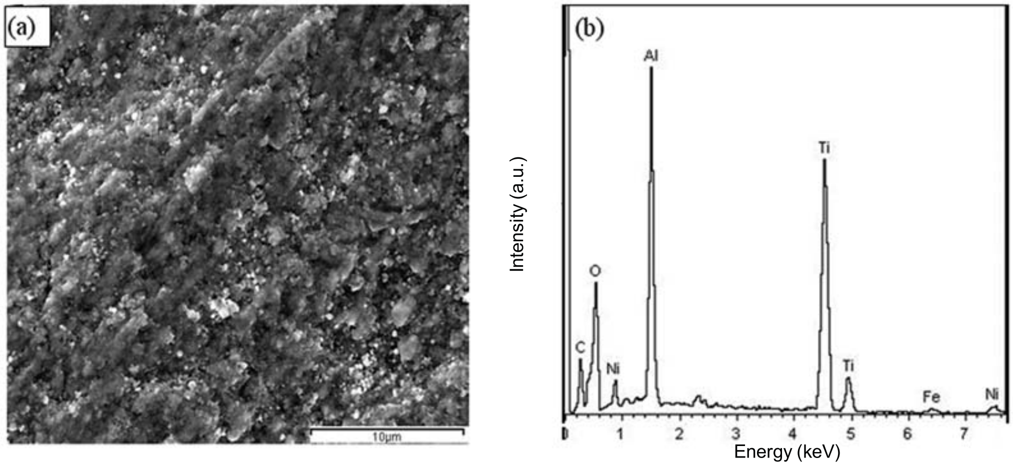

Fig. 8 SEM image (a) and EDS result (b) of the worn surface of Al_2O_3/TiC ceramic composite

The surface is seriously worn, and some pits appear because of the fallen grains and micro-cracks on the local surface. Due to the worn surface of Al_2O_3/TiC layer is seriously worn, the wear rate becomes unstable with the load increasing from 20 to 100 N under high rotational speed of 400 r/min.

3.3 Friction and wear behaviors

The worn surface of the laminated ceramic composite specimen is shown in Fig. 9. At a macroscopic scale, the worn profile of Al_2O_3/TiC/CaF_2-Al_2O_3/TiC laminated ceramic composite is varied at different layers. Several granules of the ceramic are removed from Al_2O_3/TiC layer. By contrast, Al_2O_3/TiC/CaF_2 layer maintains its original shape with no granules removed from the matrix. Fig. 9 indicates that wear mechanism is varied at different layers. Abrasive wear is the main mechanism in Al_2O_3/TiC layer as shown by the granules falling off from the worn surfaces. Adhesive wear appears to be the wear mechanism in Al_2O_3/TiC/CaF_2 layer because no granule falling off the worn surface is observed and a layer of ferric oxide is formed.

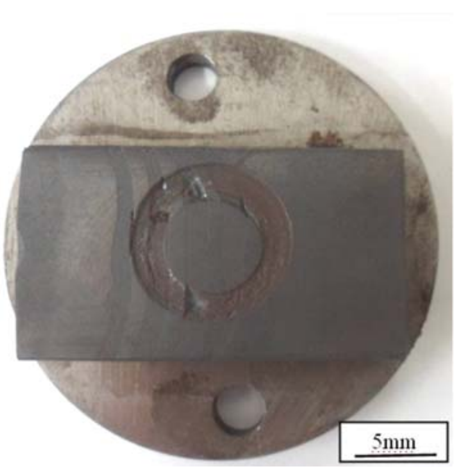

Fig. 9 Photograph of the worn surface of the tested laminated Al_2O_3/TiC/CaF_2- Al_2O_3/TiC ceramic composite

The worn surface of Al_2O_3/TiC/CaF_2-Al_2O_3/TiC laminated ceramic composite sample is shown in Fig. 10. Fig. 10(a) illustrates the worn surface of a wear-and-tear test specimen. Wear behaviors of Al_2O_3/TiC/CaF_2 and Al_2O_3/TiC layers are different. Numerous pits are formed by scraped matrix granules on the worn surface of Al_2O_3/TiC layer. By contrast, no pits are formed on Al_2O_3/TiC/CaF_2 layer. The Al_2O_3/TiC/CaF_2 matrix maintains its original appearance. The worn surface of Al_2O_3/TiC/CaF_2 layer appears to be smoother than that of Al_2O_3/TiC layer.

Fig. 10(b) shows the micrograph of the worn surface of the Al_2O_3/TiC/CaF_2 layer, wherein the worn surface is smoother than that of the Al_2O_3/TiC layer. Several adhesive materials are found on the worn surface of the Al_2O_3/TiC/CaF_2 layer. EDS result of the worn surface of the Al_2O_3/TiC/CaF_2 layer is shown in Fig. 11. Adhesive materials are ferric oxides on the worn surface. Table 2 provides a quantitative analysis of the elements corresponding micrographs of Fig. 10(b). It shows that a large amount of elements of the quenched 45 steel are found on the worn surface of the Al_2O_3/TiC/CaF_2 layer. We therefore conclude that the main wear mechanism of the Al_2O_3/TiC/CaF_2 layer is adhesive wear.

Fig. 10(c) shows the micrograph of the worn surface of the Al_2O_3/TiC layer. The worn surface is very rough and has numerous pits which are formed by falling off of the granules. EDS analysis of the worn surface of the Al_2O_3/TiC layer is shown in Fig. 12. It reveals that elements on the worn surface come mainly from the matrix and no extraneous elements are found on the worn surface. Table 2 provides a quantitative analysis of the worn surface of the Al_2O_3/TiC layer. We conclude that the wear mechanism of the Al_2O_3/TiC layer is abrasive wear. Wear resistance of the Al_2O_3/TiC layer is lower than that of the Al_2O_3/TiC/CaF_2 layer.

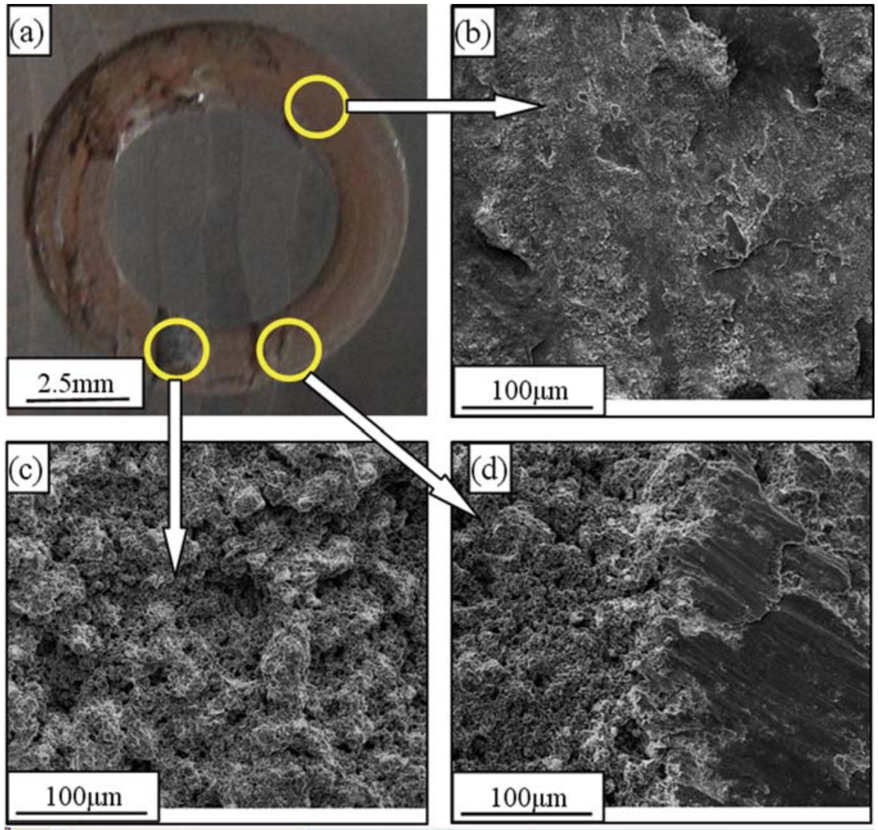

Fig. 10 Worn surfaces of the Al_2O_3/TiC/CaF_2- Al_2O_3/TiC laminated ceramic composite and its micro structures within different layers: (a) image of the worn surface after wear and tear test; (b) micrograph of the Al_2O_3/TiC/CaF_2 layer of the laminated ceramic composite; (c) micrograph of the Al_2O_3/TiC layer of the laminated ceramic composite; (d) micrograph of the junction area between the Al_2O_3/TiC/CaF_2 layer and the Al_2O_3/TiC layer

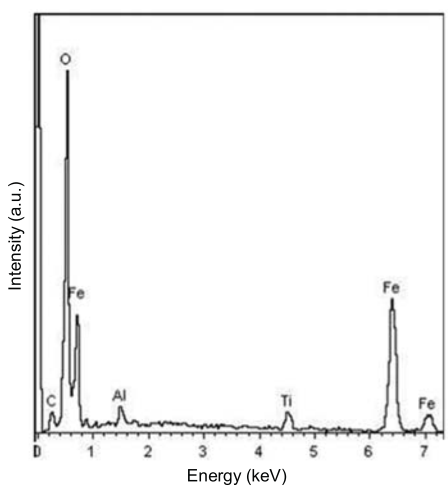

Fig. 11 EDS result of the worn surface of the tested Al_2O_3/TiC/CaF_2 layer in the laminated Al_2O_3/TiC/CaF_2-Al_2O_3/TiC ceramic composite

Fig. 10(d) shows the micrograph of the worn surface of the junction between Al_2O_3/TiC/CaF_2 and Al_2O_3/TiC layers. It is seen that friction surfaces of the main loading area on Al_2O_3/TiC/CaF_2 layers are covered with Fe. Al_2O_3/TiC/CaF_2 layers exhibiting better wear resistance than Al_2O_3/TiC layers. Wear behavior appears to be abrasive, with numerous pits resulting from granules falling off.

Fig. 13 shows the exfoliative worn surface of Al_2O_3/TiC/CaF_2 and Al_2O_3/TiC layers. Microstructures of Al_2O_3/TiC/CaF_2 layers appear to be more compact than those of Al_2O_3/TiC layers. Fig. 13(a) shows that a number of vacancies are formed on the Al_2O_3/TiC/CaF_2 layer by granules falling off on the worn surfaces. Fig. 13(b) indicates the presence of numerous holes in the matrix on the Al_2O_3/TiC layer because the matrix becomes loose without the application of pressure during sintering.

Fig. 14 shows the microstructure and EDS results of Al_2O_3/TiC/CaF_2 layers. It can be seen that Al_2O_3 and TiC appear to be large granules. CaF_2 particles

Table 2 Compositions (wt.%) of different layers in Al_2O_3/TiC/CaF_2-Al_2O_3/TiC laminated ceramic composite

Layer	C	O	F	Al	Ca	Ti	Fe	Ni	Mo
Al_2O_3/TiC/CaF_2	10.01	33.44	1.61	15.37	0.65	33.38	1.90	2.66	0.98
Al_2O_3/TiC	4.65	32.73	–	1.16	–	3.23	55.17	3.06	–

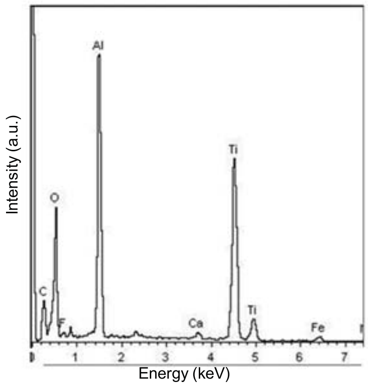

Fig. 12 EDS result of the worn surface of Al_2O_3/TiC layer in the laminated Al_2O_3/TiC/CaF_2-Al_2O_3/TiC ceramic composite (a) Al_2O_3/TiC/CaF_2 layers (b) Al_2O_3/TiC layers

exist in the gaps between the granules as the binding phase, which may be attributed to the melting temperature of CaF_2 (1450 °C). EDS of Al_2O_3, TiC, and CaF_2 are shown in Fig. 14(b), (c) and (d), respectively. Wear resistance of Al_2O_3/TiC/CaF_2 layer exceed that of Al_2O_3/TiC layer because CaF_2 is used as the binding phase. Under the selected friction load, thermal expansion coefficient of CaF_2 particles differs from that of the matrix, which caused microcracks to appear as a result of induced thermal stress. When Al_2O_3 or TiC granules fall off on the worn surfaces, the CaF_2 phase is exposed on the worn surface. As a result of low shear modulus and strength, CaF_2 particles pull and cover friction surfaces and form a self-lubricating film. This solid, self-lubricating film on the friction surface

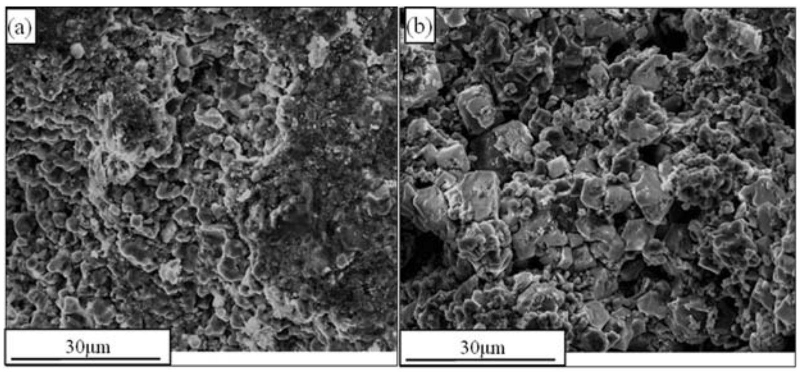

Fig. 13 SEM images of worn surfaces of Al_2O_3/TiC/CaF_2 layer (a) and Al_2O_3/TiC layer (b) in the laminated Al_2O_3/TiC/CaF_2-Al_2O_3/TiC ceramic composite

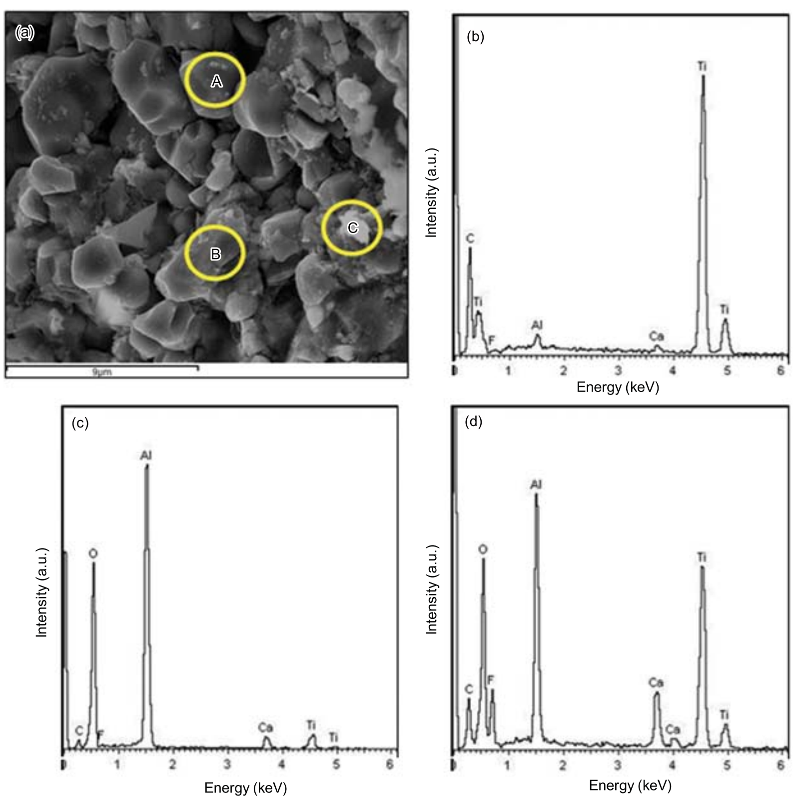

Fig. 14 SEM image of the Al_2O_3/TiC/CaF_2 layer (a) and EDS results of the position denoted by the circle A (b), circle B (c) and circle C (d) in Fig.14 (a)

makes the friction coefficient of $Al_2O_3/TiC/CaF_2$ layer lower than that of Al_2O_3/TiC layers, thereby increasing wear resistance.

3.4 Comparison of $Al_2O_3/TiC/CaF_2$- Al_2O_3/TiC laminated composite and Al_2O_3/TiC

Fig. 15 shows worn morphologies of $Al_2O_3/TiC/CaF_2$-Al_2O_3/TiC laminated composite and Al_2O_3/TiC ceramic, which were fabricated and tested under the same conditions. The wear rate of Al_2O_3/TiC ceramic is shown to be higher than that of $Al_2O_3/TiC/CaF_2$-Al_2O_3/TiC laminated composite. Therefore, wear resistance of $Al_2O_3/TiC/CaF_2$-Al_2O_3/TiC laminated composite surpasses that of Al_2O_3/TiC ceramic.

Fig. 16 presents a comparison of friction coefficients of the two studied specimens at a load of 20 N. Friction coefficient of $Al_2O_3/TiC/CaF_2$-Al_2O_3/TiC laminated composite is shown to be lower than that of Al_2O_3/TiC ceramic. As the rotational speed rises from 100 r/min to 200 r/min, average friction coefficients increase from 0.3 to 0.6. By contrast, Al_2O_3/TiC ceramic composites have a larger friction coefficient. As rotational speed increases, friction coefficient of Al_2O_3/TiC ceramic composite falls from 0.68 to 0.63. $Al_2O_3/TiC/CaF_2$ ceramic composite is clearly lower friction coefficient than Al_2O_3/TiC composites at low rotational speed.

The wear resistance of the ceramic composite is proportional to $H_V^{1/2} \cdot K_{IC}^{3/4}$, where H_V is the Vickers hardness and K_{IC} is the fracture toughness. Following Eq. (1), the wear-rate curves of $Al_2O_3/TiC/CaF_2$-Al_2O_3/TiC laminated composite and Al_2O_3/TiC under different loads are outlined in Fig. 17. When rotational speed reaches 100 r/min, $Al_2O_3/TiC/CaF_2$-Al_2O_3/TiC laminated composite and Al_2O_3/TiC composite demonstrate completely different wear characteristics. Wear rate of Al_2O_3/TiC composite tends to increase rapidly as load increases. The value rises from 4.073×10^{-11} m^2N^{-1} to 26.714×10^{-11} m^2N^{-1} when the load increases from 20 to 40 N. The wear rate of $Al_2O_3/TiC/CaF_2$-Al_2O_3/TiC laminated composite tends to decrease slightly from approximately 3×10^{-11} m^2N^{-1} to 1.28×10^{-11} m^2N^{-1} when the load increases from 20 to 40 N. A minimum wear rate is obtained at the load of 40 N. As the load further increases, wear rate increases at lower rate. Over the entire load range, wear rate of Al_2O_3/TiC composite is higher than that of $Al_2O_3/TiC/CaF_2$-Al_2O_3/TiC laminated composite, particularly under high loads.

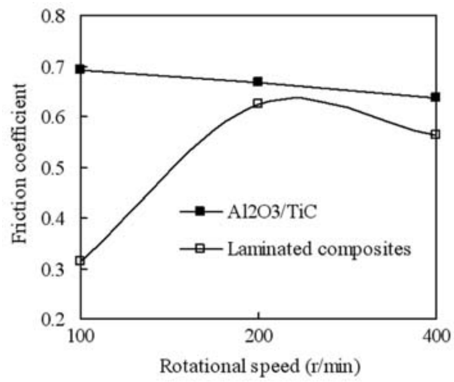

Fig. 16 Friction coefficients of the $Al_2O_3/TiC/CaF_2$-Al_2O_3/TiC laminated composite and Al_2O_3/TiC ceramic variation with rotational speed (load= 20 N)

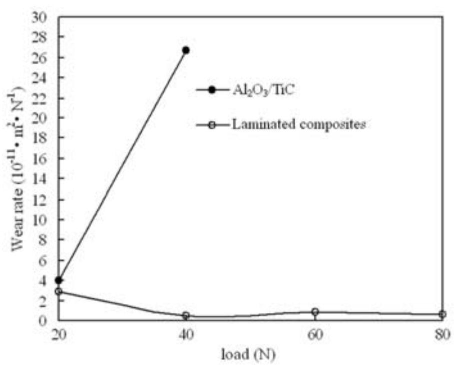

Fig. 17 Wear rates of the $Al_2O_3/TiC/CaF_2$-Al_2O_3/TiC laminated composite and Al_2O_3/TiC ceramic variation with load (rotational speed=100 r/min)

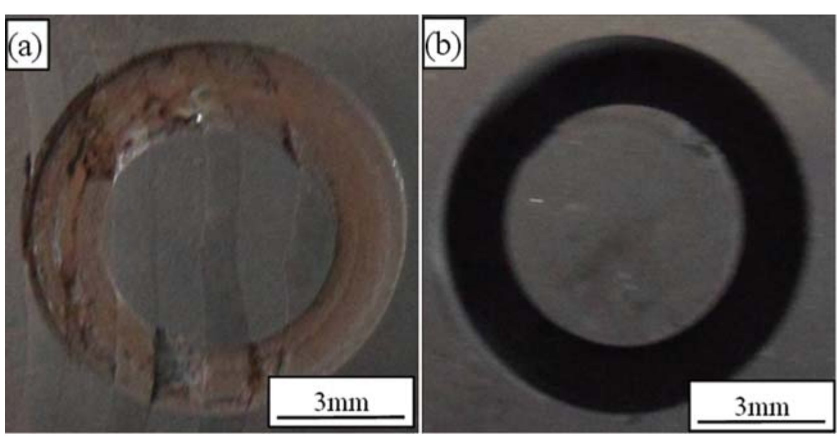

Fig. 15 Worn surfaces of $Al_2O_3/TiC/CaF_2$-Al_2O_3/TiC laminated composites (a) and Al_2O_3/TiC ceramic (b)

4. Conclusions

This paper investigated and compared wear behavior of Al_2O_3/TiC/CaF_2-Al_2O_3/TiC laminated ceramic composite and of Al_2O_3/TiC ceramic. The following findings were derived from the study:

(1) Al_2O_3/TiC/CaF_2-Al_2O_3/TiC laminated composite prepared by cold pressing and sintering, has a friction coefficient of 0.5 to 0.6, which is lower than that of Al_2O_3/TiC composite. The wear rate of the former increases with increasing friction plate rotational speed. The wear rate of the laminated composite is lower than 10×10^{-11} $m^3\cdot N^{-1}\cdot m^{-1}$, which is also lower than that of Al_2O_3/TiC composite.

(2) The wear morphologies of the Al_2O_3/TiC/CaF_2 and Al_2O_3/TiC layers of the laminated ceramic composite are different. A large number of the pits are formed by the scraped Al_2O_3/TiC matrix on the worn surface of Al_2O_3/TiC layer. The Al_2O_3/TiC/CaF_2 layer maintains its original appearance, and the worn surface of Al_2O_3/TiC/CaF_2 layer is smoother than those of Al_2O_3/TiC layer.

(3) Al_2O_3/TiC/CaF_2 layer is more compact than Al_2O_3/TiC layer in the laminated composite, and exhibits lower friction coefficient as well as higher wear resistance than Al_2O_3/TiC layer because CaF_2 is used as the binding phase. When Al_2O_3 or TiC granules fall off the worn surface, CaF_2 becomes exposed. As a result of low shear modulus and strength, tiny CaF_2 particles are pulled out and covered on friction surface to form a self-lubricating film. Because of the solid, self-lubricating CaF_2 on the friction surface, friction coefficient of Al_2O_3/TiC/CaF_2 layer is lower than that of Al_2O_3/TiC layers. The wear resistance of the former is also better than that of the latter.

(4) Friction coefficient and the wear resistance of the prepared Al_2O_3/TiC/CaF_2-Al_2O_3/TiC laminated composite are found to be better than those of Al_2O_3/TiC ceramic fabricated using the same sintering process. Al_2O_3/TiC/CaF_2-Al_2O_3/TiC laminated composites improve the worn surface and have better wear resistance than Al_2O_3/TiC ceramics.

(5) The main wear mechanism of Al_2O_3/TiC/CaF_2-Al_2O_3/TiC laminated composites differs across Al_2O_3/TiC/CaF_2 and Al_2O_3/TiC layers. The main wear mechanism of Al_2O_3/TiC/CaF_2 layer is adhesive wear, whereas of Al_2O_3/TiC layer is abrasive wear. The wear resistance and self-lubricating mechanism of Al_2O_3/TiC/CaF_2 layer are attributed to CaF_2 absorbed on friction pairs. Solid CaF_2 lubricant fills micropits and the worn area, and develops a self-lubricating film during pressure driving. This self-lubricating film enhances wear resistance and decreases friction coefficients.

Acknowledgements

This work was supported by the National Natural Science Foundation for Young Scholars of China (No. 51005100), China Postdoctoral Science Foundation (No. 20110491572) and Scientific and Technologic Development Program of Shandong Province (No. 2012GGX10324).

REFERENCES

[1] X.F. Yang, X.B. Ze, H.Y. Wang and H. Wang, Ceram. Int. **34** (2009) 3495
[2] J.J. Lu, S.R. Yang, J.B. Wang and Q.J. Xue, Wear **249** (2001) 1070
[3] K.Z. Sang, Z.L. Lü and Z.H. Jin, Wear **253** (2002) 1188
[4] M.H. Cho, J. Ju, S.J. Kim and H. Jang, Wear **260** (2006) 855
[5] G. de Portu, L. Micele, D. Prandstraller, G. Palombarini and G. Pezzotti, Wear **260** (2006) 1104
[6] M.A. El Hakim, M.D. Abad, M.M. Abdelhameed, M.A. Shalaby and S.C. Veldhuis, Tribo. Int. **44** (2011) 1174
[7] X.F. Yang, J.X. Deng, H. Wang and X. B. Ze, Trans. Nonferrous Met. Soc. China **17** (2007) s663
[8] M.S. Suh, Y.H. Chae and S.S. Kim, Wear **264** (2008) 800
[9] X.F. Yang, J.X. Deng and S.Q. Yao, J. Ceram. Soc. China **33** (2005) 1522
[10] H. Chang, J. Binner and R. Higginson, Wear **268** (2010) 166
[11] A.P. Harsha, Wear **271** (2011) 942
[12] H.M. Wang, Y.L. Yu and S.Q. Li, Scr. Mater. **47** (2002) 57
[13] M. Shuaib and T.J. Davies, Wear **249** (2001) 20
[14] J.X. Deng, L.L. Liu, X.F. Yang, J.H. Liu and J.L. Sun, Mater. Des. **28** (2007) 757
[15] J.X. Deng, T.K. Cao, X.F. Yang, J.H. Liu and J.L. Sun, Ceram. Int. **33** (2007) 213
[16] J.H. Ouyang, Y.F. Li, Y.M. Wang, Y. Zhou, T. Murakami and S. Sasaki, Wear **267** (2009) 1353
[17] V. Fox, A. Jones, N.M. Renevier and D.G. Teer, Surf. Coat. Technol. **125** (2000) 347
[18] N.M Renevier, N. Lobiondo, V.C Fox, D.G Teer and J. Hampshire, Surf. Coat. Technol. **123** (2000) 84
[19] S.M. Patrick, P. Randyka and C.F. Higgs, Wear **272** (2011) 122
[20] J.V. Pimentel, T. Polcar and A. Cavaleiro, Surf. Coat. Technol. **205** (2011) 3274
[21] K. Rajkumar and S. Aravindan, Tribo. Int. **44** (2011) 347
[22] A. Tarlazzi, E. Roncari, P. Pinasco, S. Guicciardi, C. Melandri and G. de Portu, Wear **244** (2000) 29
[23] J.M. Carrapichano, J.R. Gomes and R.F. Silva, Wear **253** (2002) 1070